Arcuate fasciculus architecture is associated with individual differences in pre-attentive detection of unpredicted music changes

Lucía Vaquero [a,*], Neus Ramos-Escobar [b,c], David Cucurell [b,c], Clément François [c,d], Vesa Putkinen [e], Emma Segura [b,c], Minna Huotilainen [f], Virginia Penhune [g,h,i], Antoni Rodríguez-Fornells [b,c,j]

[a] Laboratory of Cognitive and Computational Neuroscience, Complutense University of Madrid and Polytechnic University of Madrid, Campus Científico y Tecnológico de la UPM, Pozuelo de Alarcón, 28223 Madrid, Spain
[b] Department of Cognition, Development and Education Psychology, and Institute of Neurosciences, University of Barcelona, Barcelona, Spain
[c] Cognition and Brain Plasticity Unit, Bellvitge Biomedical Research Institute (IDIBELL). L'Hospitalet de Llobregat, Barcelona, Spain
[d] Aix Marseille Univ, CNRS, LPL, Aix-en-Provence, France
[e] Turku PET Centre, University of Turku, Turku, Finland
[f] Cicero Learning and Cognitive Brain Research Unit, University of Helsinki, Helsinki, Finland
[g] Penhune Laboratory for Motor Learning and Neural Plasticity, Concordia University, Montreal, QC, Canada
[h] International Laboratory for Brain, Music and Sound Research (BRAMS). Montreal, QC, Canada
[i] Center for Research on Brain, Language and Music (CRBLM), McGill University. Montreal, QC, Canada
[j] Institució Catalana de recerca i Estudis Avançats (ICREA), Barcelona, Spain

ARTICLE INFO

ABSTRACT

The mismatch negativity (MMN) is an event related brain potential (ERP) elicited by unpredicted sounds presented in a sequence of repeated auditory stimuli. The neural sources of the MMN have been previously attributed to a fronto-temporo-parietal network which crucially overlaps with the so-called auditory dorsal stream, involving inferior and middle frontal, inferior parietal, and superior and middle temporal regions. These cortical areas are structurally connected by the arcuate fasciculus (AF), a three-branch pathway supporting the feedback-feedforward loop involved in auditory-motor integration, auditory working memory, storage of acoustic templates, as well as comparison and update of those templates. Here, we characterized the individual differences in the white-matter macrostructural properties of the AF and explored their link to the electrophysiological marker of passive change detection gathered in a melodic multifeature MMN-EEG paradigm in 26 healthy young adults without musical training. Our results show that left fronto-temporal white-matter connectivity plays an important role in the pre-attentive detection of rhythm modulations within a melody. Previous studies have shown that this AF segment is also critical for language processing and learning. This strong coupling between structure and function in auditory change detection might be related to life-time linguistic (and possibly musical) exposure and experiences, as well as to timing processing specialization of the left auditory cortex. To the best of our knowledge, this is the first time in which the relationship between neurophysiological (EEG) and brain white-matter connectivity indexes using DTI-tractography are studied together. Thus, the present results, although still exploratory, add to the existing evidence on the importance of studying the constraints imposed on cognitive functions by the underlying structural connectivity.

1. Introduction

A crucial trait for survival in humans and other species is the capacity to constantly monitor the environment in order to notice unpredicted sensory changes. Whenever an auditory stimulus differs from the previous expected ones, a frontal negative component of the Event-Related brain potentials (ERP), the Mismatch Negativity (MMN),

can be observed (Picton et al., 2000). The MMN is evoked in the context of the presentation of a sequence of repeated stimuli, when the expected sequence is broken or altered in its sound characteristics by the appearance of a less probable stimulus that varies in a particular feature (intensity, frequency, duration, interstimulus interval, etc.), a combination of features, the presentation of more complex patterns, or the absence of an expected part of the pattern (Horváth et al., 2010; Grotheer and Kovács, 2016; for reviews see Näätänen et al., 2005; Grimm and Escera, 2012). The MMN has been thus proposed to reflect the pre-attentive detection of a discrepancy between the features of the incoming sound and those predicted based on the preceding auditory

input (Näätänen et al., 2007; Winkler et al., 2009; Koelsch et al., 2018). This memory trace is postulated to be used as an internal template against which incoming sensory information is compared.

The contribution of prefrontal neural generators to the MMN has been demonstrated by both classic EEG investigations (Näätänen et al., 1978; Frodl-Bauch et al., 1997), as well as more recent studies using current source density analyses, and combined functional magnetic resonance imaging (fMRI) and magnetoencephalography (MEG) (Alho et al., 1996; Doeller et al., 2003; Giard et al., 1990; Maess et al., 2007; Opitz et al., 2002). The involvement of frontal generators has been further confirmed by studies of frontal-lobe lesions patients (Alho et al., 1994; Alain et al., 1998). Based on these studies, the neural sources of the MMN may involve three main regions. (i) The primary and secondary auditory regions within the superior temporal gyrus (STG, Szycik et al., 2013; Halgren et al., 1995). (ii) The inferior (IFG) and middle frontal gyri, and prefrontal areas (Doeller et al., 2003; Maess et al., 2007; Lappe et al., 2013; Szycik et al., 2013) which play an important role in sustained attention, object recognition, and auditory working memory comparing acoustic inputs with established sensory templates, and which have been described as involved in the detection of syntactic and harmonic violations (Koelsch et al., 2006; Sammler et al., 2011). (iii) The inferior parietal regions (IPG) which are involved in temporal processing and building up on-line expectations (Lappe et al., 2013). Interestingly, the MMN temporal sources have been also reported to have a leftward asymmetry for linguistic stimuli (Näätänen et al., 1997) and a rightward asymmetry for musical ones (Tervaniemi et al., 1999). Further, the MMN is right lateralized for melodic deviants and more bilaterally distributed for rhythmic deviants (Lappe et al., 2013). Nonetheless, the exact roles of the different MMN-source regions remain controversial. In addition, other ERP components are elicited as well after deviant responses, especially the frontal P3a. This component has been associated with the process of involuntary attention capture by target stimulus and the process of attention shifting toward the surprising sound (Nager et al., 2003; Horváth et al., 2008; Berti, 2013).

The proposed generators of the MMN component are organized along the dorsal auditory stream, likely because this pathway provides a direct link and supports a temporally precise bidirectional flow of information between auditory and motor planning regions (Patel and Iversen, 2014), allowing feedback monitoring, creation of predictions and error correction (Hickok and Poeppel, 2007; Rauschecker and Scott, 2009). The dorsal stream regions are anatomically linked by the arcuate fasciculus (AF), a white-matter pathway connecting IFG and prefrontal areas (including parts of ventral premotor and middle frontal cortices) with STG, temporo-parietal and IPG regions (Hickok and Poeppel, 2007; Rauschecker and Scott, 2009; Patel, 2014; Vaquero et al., 2017, 2018). The anatomical properties of the brain may drive the nature of information processing (Behrens and Johansen-Berg, 2005), and, in turn, the functional differences may lead to anatomical variation. Thus, individual differences observed at the functional level as reflected by the MMN should be associated with the underlying anatomical dorsal circuitry and, in particular, with individual differences in the local white matter conveying information across these regions. In addition, the AF is thought to sustain the fast feedback-feedforward loops that allow the creation of temporary predictions based on the integration of multisensory information and its comparison with previous auditory templates (Cunillera et al., 2009; Lopez-Barroso et al., 2013; Rodríguez-Fornells et al., 2009; Brown et al., 2015; Vaquero et al., 2017, 2018). Due to this auditory-motor coupling interface and fast feedback-feedforward loops, the AF has been proposed to be a crucial structure in music learning, especially during its initial stages in which feedback and motor corrections are vital to improving performance (Kleber et al., 2013; James et al., 2014; Mamiya et al., 2016). Recent evidence supports this hypothesis by showing the important involvement of the right AF in music learning (Brown et al., 2015; Loui, 2015), even in individuals without musical training (Vaquero et al., 2018).

In the current exploratory study, we used, for the first time, diffusion tensor imaging (DTI) to characterize the white matter properties of the neural network involved in the generation of the MMN in 26 adults. DTI can provide information on the structural organization of the white-matter fibers. Specifically, our DTI marker of interest was tract-volume, which is thought to reflect fiber-packing properties, the thickness and morphology of myelin sheaths, astrocyte and oligodendrocyte density, and the vasculature architecture surrounding the tracts (Juraska and Markham, 2004; Tham et al., 2011; Zatorre et al., 2012; Frintrop et al., 2018; Zhang et al., 2017). Thus, tract volume is a white-matter marker that provides information about the organization of the anatomical connectivity essential for the integration and transmission of neural information across spatially separated cortical regions, such as the MMN sources. For instance, a better structural organization might likely reflect increased efficiency in transmitting information, higher nerve conduction velocities due to greater myelination, better fiber packing, and/or an increased probability of transmission along an axon that might facilitate a wide-scale synchronization of signals across distant neural networks (Fields, 2008; Zatorre et al., 2012). Because ERPs are mainly generated by the summation of graded postsynaptic potentials on cortical pyramidal neurons (Elul, 1971; Purpura, 1959; Varela et al., 2001), differences in the structural organization in areas or tracts involved in the generation of the ERPs might lead to differences in their latency (Cardenas et al., 2005) or amplitude (Westlye et al., 2009; see also for discussion, Rykhlevskaia et al., 2008; Sui et al., 2014; Valdés-Hernandez et al., 2010(Valdés-Hernández, 2010)).

The main goal of the present study was thus to examine the association between the macrostructural properties of the arcuate fasciculus and the amplitude and latency of the MMN during the melodic multi-feature paradigm (Tervaniemi et al., 2014, 2016). We decided to explore the neurophysiological-structural relationship in the context of a musical MMN paradigm in non-musicians because previous reports have consistently reported that musicians present an enhanced response to musical deviants in MMN ERP paradigms compared to non-musicians (Fujioka et al., 2004(Fujioka, 2004); Nikjeh et al., 2009(Nikjeh, 2009); Vuust et al., 2012(Vuust, 2012); Putkinen et al., 2014; Virtala et al., 2014(Virtala, 2014); but see Paraskevopoulos et al., 2011(Paraskevopoulos, 2012)). Therefore, in the present study we aimed to explore possible structural-functional relationships in general population, which we assume is mostly constituted by non-musicians. Based on the rationale explained above, individuals without music training but with a better macrostructural organization of their AF would be expected to show better automatic change detection on our music-related MMN paradigm. Further, according to previous reports, we hypothesized that MMN- and P3a-related measures for rhythm/timing deviants would be associated with macrostructural properties of the left or bilateral AF, while electrophysiological measurements for melodic/pitch deviants would be related to the right AF (Grahn and Brett, 2007; Zatorre et al., 2007; Lappe et al., 2013; Strauß et al., 2014; Vaquero et al., 2018).

2. Materials and methods

2.1. Participants

The present investigation was carried out in a subsample of participants that participated in a previously published study exploring rapid music learning in non-musicians (see Vaquero et al., 2018). This subsample was composed of 26 individuals (out of 44) who accepted to complete the EEG session in addition to the music training protocol detailed in the aforementioned study. The EEG session took place always before the music training session for all participants except for 1 who performed it one week afterwards and 5 subjects that completed it 3 years later. All participants included in the present report were healthy young right-handed non-musicians (17 females; mean age: 21 ± 1.50),

most of them university students (mean years of education: 15 ± 1.82). None of them reported any auditory, neurological or psychiatric disorder. Non-musician status was characterized via a self-report questionnaire. None of them were currently playing an instrument or singing, although all of them had attended the mandatory music lessons during primary and secondary school (around 2 h per week). The inclusion criteria in this domain were, thus, having less than 3 years of music training at least 10 years ago, or less than 1 consecutive year of training if it happened less than 10 years ago; all participants satisfied the inclusion criteria (mean years of individual music lessons: 0.34 ± 0.93). Participants were also tested for Amusia using the Montreal Battery of Evaluation of Amusia (MBEA, Peretz et al., 2003), and none scored below the cut-off of 23. All participants were unfamiliar with the hypothesis of the study, gave their written informed consent, and received monetary compensation for their time. The procedures of this study were approved by the Ethics Committee of the Hospital Universitari de Bellvitge, Barcelona (PR181/13), and the study was conducted according to the principles of the Declaration of Helsinki.

2.2. Experimental procedure

Participants first completed an MRI session in which T1-weighted and DTI data were acquired (Alomar Medic centre, Barcelona, Spain) and, on a different day and always after the MRI session, they underwent an EEG session. The EEG session was conducted in an experimental room at the University of Barcelona containing the EEG equipment, a PC, and a monitor on which the task was presented, and a comfortable chair in which participants were seated for the whole session.

2.3. EEG session details, stimuli & analyses

2.3.1. EEG recordings

The electroencephalographic (EEG) signal was recorded from the scalp using tin electrodes mounted in an elastic cap (Electro-Cap International, International 10–20 System locations) and located at 29 standard positions (Fp1/2, Fz, F3/4, F7/8, Fcz, Fc1/2, Fc5/6, Cz, C3/4, Cp1/2, Cp5/6, T7/8, Pz, P3/4, P7/8, PO1/2 Oz) (Jasper, 1958) using a professional BrainAmp System (Brain Products) and a PC. Biosignals were referenced on-line to an electrode placed in the outer canthus of the right eye and posteriorly re-referenced off-line to the mean activity of the left and right mastoidal electrodes. Electrode impedances were kept below 5 kΩ. For all participants' experimental sessions, vertical eye movements were monitored with an electrode located at the infra-orbital ridge of the right eye. The continuous data was recorded at a sampling rate of 250 Hz and stored offline for later analysis.

To ensure that the attentional focus of the participants during the EEG-MMN protocol was not on the auditory stimuli evoking the registered MMN response, participants were presented with a silent excerpt of the movie "Modern Times" (Charles Chaplin, 1936) while the auditory stimuli (i.e., the melodic multi-feature MMN paradigm, see details below) were presented via headphones and the volume was adapted to a comfortable level for each participant. Participants were instructed to pay attention solely to the details of the movie and were informed about a short test concerning the action of the movie that took place at the end of the EEG session and served as a proxy of their attention to the visual stimuli. The test about the film contained 10 questions and all participants scored 8 – 10, which suggests participants' attention was indeed on the film.

2.3.2. EEG stimuli: melodic multi feature MMN paradigm

The stimuli consisted of 360 brief melodies composed by MH; they have been used in previous reports (Tervaniemi et al., 2014, 2016) and described in more detail by Putkinen et al. (2014). The short melodies were played using digital recordings of acoustic piano tones (from McGill University Master Samples) that respected the Western tonal rules and were recursively repeated. Short melodies started with a triad

(300 ms) followed by four tones varying in length, with a 50-ms gap between each tone and followed then by a final tone whose duration was 575 ms. Every melody lasted for 2100 ms, and there was a 125 ms gap between each melody. Melodies were presented in total for 15 min in a looped manner.

Six different deviants were included in the short melodies. These deviants can be divided into low-level (i.e., no change in the melody) and high-level (i.e., altering the melodic contour) changes and one melody could contain more than one deviant or change. See Fig. 1 for an illustration of the melodies and its possible deviants.

The three types of low-level changes were: (i) *Mistuning*: consisted of changing the pitch of a tone half of a semitone upwards, 3% of the fundamental frequency of the original sound, in 20% of the melodies. (ii) *Timbre deviant*: the timbre of a tone would be flute instead of the original digital piano timbre, in 16% of the melodies. (iii) *Rhythm mistake* or *Timing delay*: consisting of a 100 ms silence gap, in 17% of the melodies (Tervaniemi et al., 2014).

High-level changes had also three types: (i) *Melody modulation*: presented as a pitch change in the third or fourth tone of the melody, in 22% of the melodies (it lightly changed the prevailing melody and continued until a new melody modulation was presented). (ii) *Rhythm modulation*: consisting on introducing the reversal of the duration of two sequential tones, meaning that a long tone was replaced by a short one (shortening) and a short tone was replaced by a long tone (lengthening); could happen in the second or third tone, in 22% of the melodies. (iii) *Transposition, or Key change*: transposing the whole melody one semitone up or down, in 26% of the melodies (after a chord transposition, the following melodies retained the converted key until a new Transposition deviant was introduced).

All high-level changes were musically plausible, so the resulting melodies were in key and consonant, like the other variants of the melody. Moreover, high-level deviations became the new repeated form of the melody in the subsequent presentations (the following melodies were repeated in the modulated form) in a roving-standard fashion (Cowan et al., 1993). In line with this, the rhythm modulations resulted in maintaining the beat of the repeated melodies while the melody modulations resulted in the new tones belonging to the original key. Only one deviant of the same type could occur within a single melody and only one deviant could occur in a single tone. After each melody modulation, rhythm modulation, or transposition, the new 'standard' melodic or rhythmic pattern, or key was repeated at least once (approximately three repetitions on average) before the next change of the same type.

2.3.3. EEG analyses

The data was pre-processed and analysed with MATLAB R2019b (MathWorks, Inc) using ERPLAB (version 6.1.4) (Lopez-Calderon & Luck, 2014) and customized scripts. Continuous data was epoched into segments of 900 ms time-locked at the stimulus presentation, considering a 100 ms pre-stimulus baseline. Each epoch was visually inspected to identify and remove bad channels and muscular-activity artifacts.

To explore only reliable differences between standard and deviant ERP responses, as well as to properly control for Type I errors within the multiple comparisons carried out (Kilner, 2013), the ERPs from each of our six conditions were submitted to a repeated measures, two-tailed permutation test based on the tmax statistic (Blair and Karniski, 1993), using a family-wise alpha level of 0.05 by means of the Mass Univariate ERP Toolbox (Groppe et al., 2011). A time window between 50 and 350 ms was used based on the existing literature on MMN and P3a components (Tervaniemi et al., 2014; Vuust et al., 2016; Petersen et al., 2020), as performed in previous reports applying similar methodological approaches (Sanchez-Carmona et al., 2016; Scheer et al., 2016; Campos-Arteaga et al., 2020). Within the selected time-window, all time points at all 29 scalp electrodes were included in the test (i.e., 5226 total comparisons). 2500 random within-participant permutations of the data were applied to estimate the distribution of the null hypothesis (i.e., no difference between standard and deviant). Based on this esti-
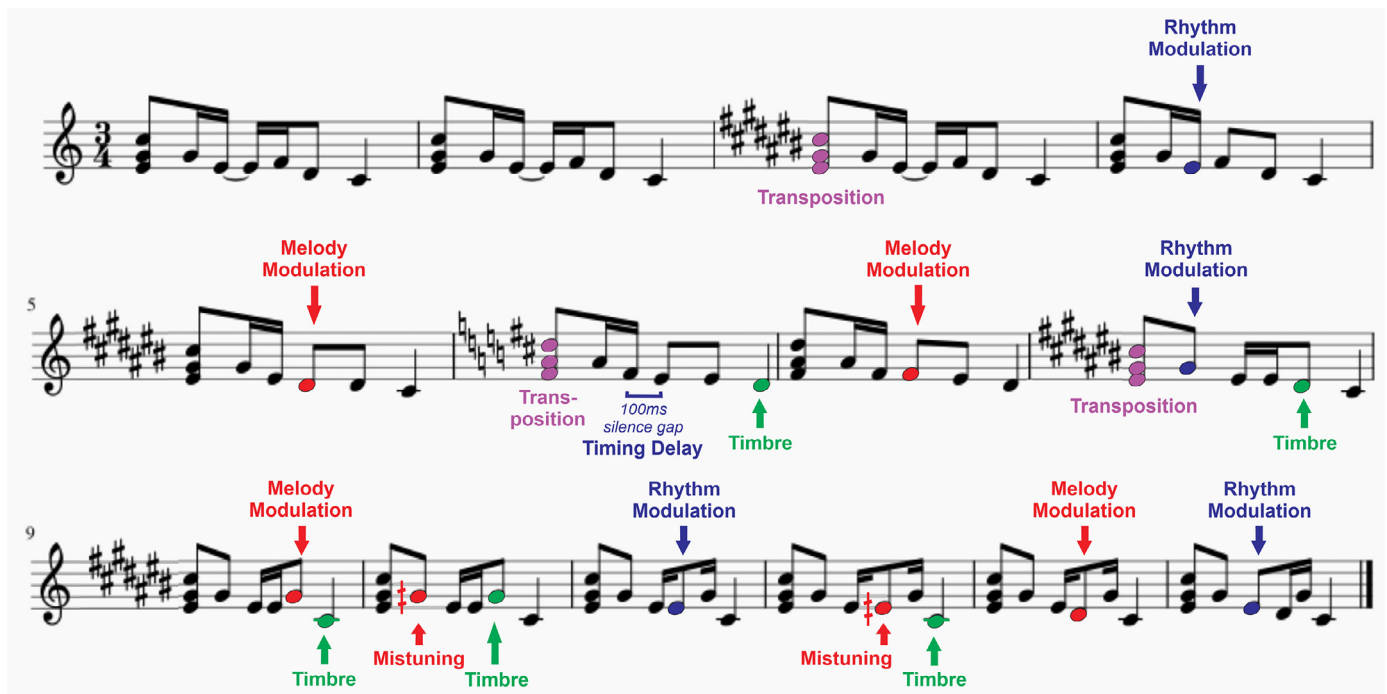
Fig. 1. Stimuli from the Melodic Multi-feature MMN paradigm. Arrows pointing down show high-level changes (i.e., Melody modulation, Rhythm modulation, Transposition / Key change); arrows pointing up show low-level deviations (i.e., Mistuning, Timbre deviants, Timing delay / Rhythm mistake).

mate, critical t-scores (df = 25) were derived. Differences in the original data for each condition's comparison that exceeded this critical t value were deemed reliable (Manly, 1997; Hemmelmann et al., 2004). Hence, in the current context, the largest negative response within our selected time-window after the presentation of the deviant stimuli was considered a MMN (Näätänen et al., 1978), while a reliable positive response following the MMN (i.e., 50–350 ms post deviant stimuli presentation) was considered a P3a (Escera et al., 2000; Friedman et al., 2001).

After examining the permutation results, the difference amplitude value (deviant–standard) relative to the 100 ms pre-stimulus baseline was calculated for the significant regions of interest (ROIs) observed, being specifically: a fronto-central cluster for the MMN elicited by all conditions (F3, Fz, F4, FC1, FCz, FC2, C3, Cz, C4), a small midline cluster for the P3a associated to the Timbre Deviant condition (Fz, FCz, Cz), and a central cluster corresponding to the P3a elicited by the Rhythm Mistake/Timing Delay condition (FC1, FCz, FC2, C3, Cz, C4, Cp1, Cp2). During the depiction of the figures, and only for display purposes, a second order low pass Butterworh IRR filter (half amplitude cut-off at 25 Hz, 12 dB/octave roll-off) was applied to the grand average of each condition.

On the other hand, to calculate the latency values of each condition, the individual ERP amplitudes were quantified for each participant by calculating the difference waveform for each condition (deviant–standard). For each difference wave, the largest peak between 50 and 350 ms was obtained for each participant and condition at the Fz electrode. After peak definition, peak latency values were obtained for both MMN and P3a (when present) components for the 6 conditions.

2.4. MRI-DTI acquisition and analyses

Diffusion Tensor Imaging (DTI: spin echo diffusivity sequence) data was acquired in a 3.0 T Discovery mr750w General Electric scanner. The DTI sequence parameters were: TR = 12,825.00 ms, TE = 9 ms; FOV = 128 × 128 × 57 mm; matrix size = 128 × 57; slice thickness = 2.0 mm; no gap; 57 axial slices; voxel size was 2 × 2 × 2 mm. Diffusion was measured along 72 non-collinear directions, using a b value
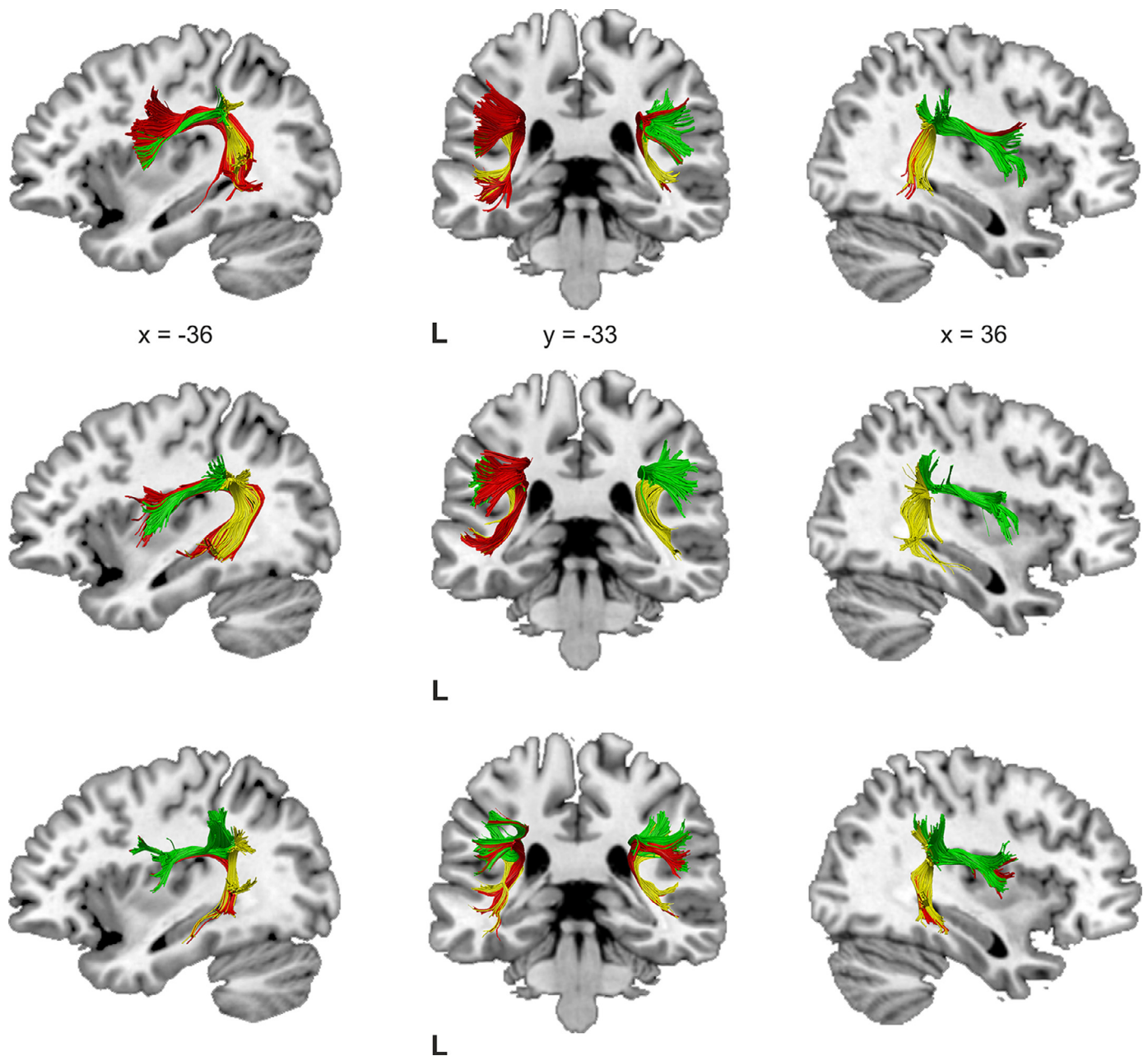
of 1000s/mm2, and including a $b = 0$ as the first volume of the acquisition as well as 8 additional $b = 0$ intercalated each 8 vol.

DTI data was not usable in 2 participants that had to be removed from the analysis. To pre-process the diffusion-weighted images of the rest of the sample ($n = 24$), first, the brain was virtually extracted from the rest of the head using FSL's Brain Extractor Tool (Smith, 2002; Smith et al., 2004; Woolrich et al., 2009). Then, motion and eddy-current correction was performed using FMRIB's Diffusion Toolbox (FDT), part of the FMRIB Software Library (FSL 5.0.1 www.fmrib.ox.ac.uk/fsl/). The b-vectors gradient matrix was then rotated to take into account the corrections made at the previous stage, by using the *fdt_rotate_bvecs* software included in the FMRIB Software Library. After this, the diffusion tensors were reconstructed using Diffusion Toolkit's least-square estimation algorithm for each voxel, and Fractional Anisotropy (FA) was calculated (Diffusion Toolkit 0.6.2, Ruopeng Wang, Van J. Wedeen, Martinos Center for Biomedical Imaging, Massachusetts General Hospital, http://www.trackvis.org/).

Deterministic tractography across the whole brain was performed in Diffusion Toolkit, using an interpolated streamlines algorithm, with 35° as the maximum curvature threshold and a minimum FA threshold of 0.2. The fibre direction is assumed here to correspond to the principal eigenvector (the eigenvector with the largest eigenvalue). This vector was color-coded (green for anterior-posterior, blue for inferior–superior and red for left-right directions) in order to generate a color–coded FA map. Dissections were carried out in the native space of each subject and in both hemispheres, by using Trackvis software (Trackvis 0.6.). The regions of interest (ROIs) were defined on the FA and FA color-coded maps according to individual anatomical landmarks. Basing and adapting the dissections on each subject's anatomy has the advantage of taking into account individual differences that can be neglected in atlas-based approaches (López-Barroso et al., 2013).

The three segments of the AF were dissected by LV using three manually defined ROIs as described in previous studies (Catani et al., 2005, 2007; López-Barroso et al., 2013; Vaquero et al., 2017, 2018). In detail, the first ROI was delineated in the coronal view, anterior to the central sulcus, encompassing the fibres going to the inferior frontal gyrus

Fig. 2. Arcuate fasciculus dissection examples. Dissections of three participants are displayed on top of a T1-weighted template. MNI coordinates are provided. Red fibers correspond to the Long or direct segment, green fibers are the Anterior segment, and yellow fibers belong to the Posterior segment. Please note the inter-individual differences in the shape and size of the different segments across the three subjects. The individual at the top row is clearly left-lateralized but possesses a thin right long segment; the participant in the middle row is strongly left-lateralized, meaning that s/he does not present a right long segment; the individual at the bottom row seems quite symmetrically distributed. Abbreviations: L, left hemisphere.

(IFG, including: Brodmann's areas 44 and 45, and parts of the medial frontal gyrus). Then, in the axial view, a second ROI was drawn covering the white matter underlying the superior and medial temporal gyrus (STG, embracing the fibers traveling to Brodmann's areas 22p, 41 and 42). Finally, the third ROI was depicted on the sagittal view, covering supramarginal and angular gyri and including the fibers traveling to the inferior parietal lobe (IPL, Brodmann's areas 39 and 40). These ROIs were combined to define the three rami of the AF: the long or direct (between IFG and STG areas), the anterior (linking IFG and IPL territories) and the posterior (connecting STG and IPL regions) segments. When needed, artefactual fibers were removed using exclusion ROIs. See Fig. 2 for examples of the AF dissections in several of our participants.

2.5. Statistical analysis

It is important to emphasize that the present is an exploratory study, with no a-priori concerning the relationship between the structural and the neurophysiological information. Regarding the DTI part of the analysis, we restricted our statistical correlational analysis to tract volume measures since previous investigations have shown that this white-matter (WM) parameter is very sensitive to individual differences in healthy individuals (Vaquero et al., 2017, 2018). Tract volume informs about the macrostructural organization of the tract, including its packing properties, myelin sheath's morphology and surrounding vascular architecture (Juraska and Markham, 2004; Zatorre et al., 2012;

Table 1

Relationship between the neurophysiological variables (MMN and P3a cluster values). Results in bold font show the significant correlation. All values are rounded to a maximum of two decimals, and only those correlations with $r \geq 0.25$ are shown.

	Melody Modulation MMN Amplitude	Rhythm Modulation MMN Amplitude	Timbre Deviant MMN Amplitude	Timbre Deviant P3a Amplitude	Rhythm Mistake MMN Amplitude
Rhythm Modulation MMN Amplitude					
Timbre Deviant MMN Amplitude	r = 0.28 p = .16	r = −0.25 p = .22			
Timbre Deviant P3a Amplitude	r = 0.25 p = .22	r = −0.26 p = .20			
Rhythm Mistake MMN Amplitude	**r = 0.57*** **p < .005**		r = 0.30 p = .13		
Rhythm Mistake P3a Amplitude				r = 0.32 p = .11	

Zhang et al., 2017). We, thus, extracted the volume from the three rami of the AF in each hemisphere.

For the EEG part of the analyses, the amplitude values corresponding to the significant clusters obtained in the permutation analyses of the different MMN conditions were multiplied by −1, changing almost all the values to positive ones, which makes easier the interpretation of the results from the correlational analysis. Importantly, the clusters obtained from the t-max permutation-based analyses were family-wise corrected, which confers good reliability and strength to the neurophysiological data used to perform the correlation with the anatomical measurements.

Pearson correlations between the WM related measurements and the values derived from the MMN-paradigm (i.e., MMN amplitude and MMN latency, as well as P3a –amplitude and latency–, if present) were performed. These correlations were run using IBM SPSS Statistics 25 (IBM Corp. Released 2017. IBM SPSS Statistics for Windows, Version 25.0. Armonk, NY: IBM Corp.). FDR-corrections were then performed by condition (4 deviant conditions with 2–4 variables each –*MMN amplitude, MMN latency, P3a amplitude, P3a latency*–; 2 hemispheres, 3 AF segments with 1 structural variable each –*Long, Anterior, and Posterior volume*–) using Matlab 2017a (fdr_bh.m, by David M. Groppe & D.H.J. Poot). Thus, correlations were considered significant for *p*-values below 0.05 after FDR correction with $n = 12$ comparisons for Melody modulation and Rhythm modulation conditions, and $n = 18$ comparisons for Timbre deviant and Rhythm Mistake conditions. Non-FDR corrected results were considered interesting trends and, thus, are also reported below. *P*-values were adjusted for non-sphericity using the Greenhouse-Geisser test when appropriate.

3. Results

3.1. EEG results

MMN components were found for all conditions except for Mistuning and Transposition/Key Change. Responses to the different melody violations, accompanied by the raster plots showing the significant clusters of electrodes and time-widows for each condition, are illustrated in **Fig. 3**. As the figure shows, the amplitude and robustness of the MMN component for the Mistuning and the Transposition/Key change conditions did not exceed the critical *t*-value calculated during the permutation analysis and, thus, those two components were not included in the correlational analysis.

The relationship between MMN and P3a amplitudes within their significant cluster for the final 4 conditions included in the correlations, were estimated to test if any of the conditions overlapped. We found a significant relationship between the cluster values corresponding to the MMN amplitude for Melody Modulation and the ones for Rhythm Mistake. Details of these correlations can be consulted in **Table 1**.

It is important to highlight that, as previously stated, participants were not paying attention to the auditory stimuli, so we were able to capture the pre-attentive brain responses to the acoustic deviants. This lack of voluntary attention to the acoustic stream was ensured thanks to the questionnaire regarding the action in the "Modern Times" film excerpt and to the fact that subjects did not show a P3a component in every deviant, which would have appeared in case they directed their attention consciously towards the acoustic changes in the stimuli.
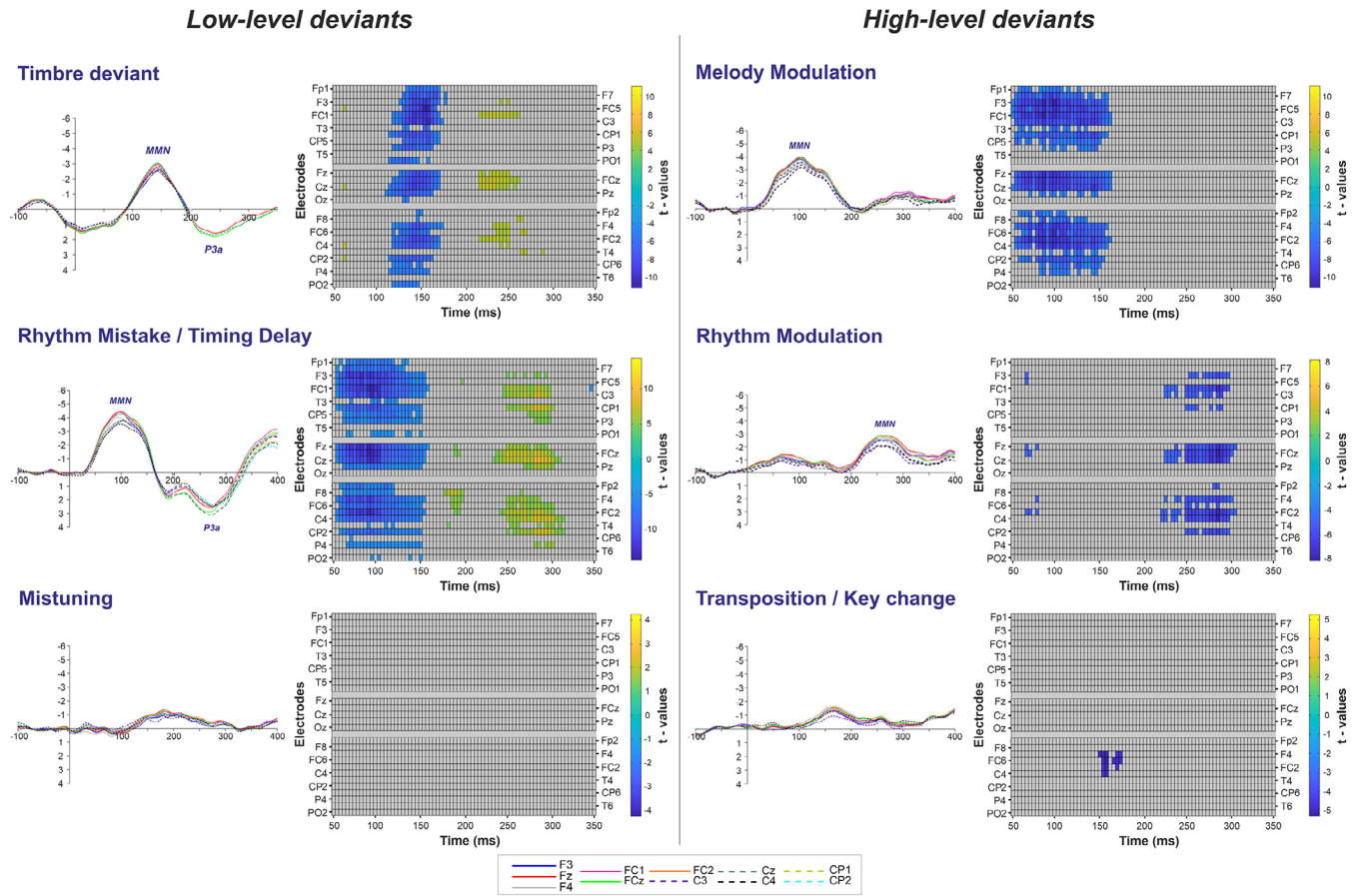
3.2. DTI results

In addition to the 2 participants with non-usable DTI data, the left Long segment of one participant was not identified and, as it is standard practice in the deterministic reconstruction of this tract (Catani et al., 2005), this subject was as well removed from the analysis. Removal of complete subjects due to a missing left long segment has been extensively performed in previous reports applying Catani's methods of reconstruction of the AF (López-Barroso et al., 2013; (Vaquero et al., 2017), 2018, 2020(Vaquero, 2020)). The explanation behind this kind-of-radical approach is that, in most right-handed individuals, the long segment constitutes the strongest left-lateralized branch regarding its volume (Thiebaut de Schotten et al., 2011), being always the thickest (counting the 6 branches from both hemispheres) and thus, when one cannot find it on the left, a deeply different white-matter architecture is supposed for that subject. So, in order not to include 'outliers' regarding right-handed subject's brain organization, data from these individuals is completely removed from the analysis. As a consequence, the right long segment is usually quite thin or even missing, and that is accepted as 'normal'. The indirect segments (anterior and posterior) are usually missing in one of the hemispheres in a small proportion of individuals (Catani and Mesulam, 2008). Hence, the AF was detected bilaterally in the rest of the sample ($n = 23$) with the usual frequency of a small number of missing segments: the right Long segment was missing in 8 participants (34.8%, $n = 15$), and the right Anterior segment was not detected in one participant (4.4%, $n = 22$). Due to this issue, correlations were explored for each segment for the final set of 23 participants.
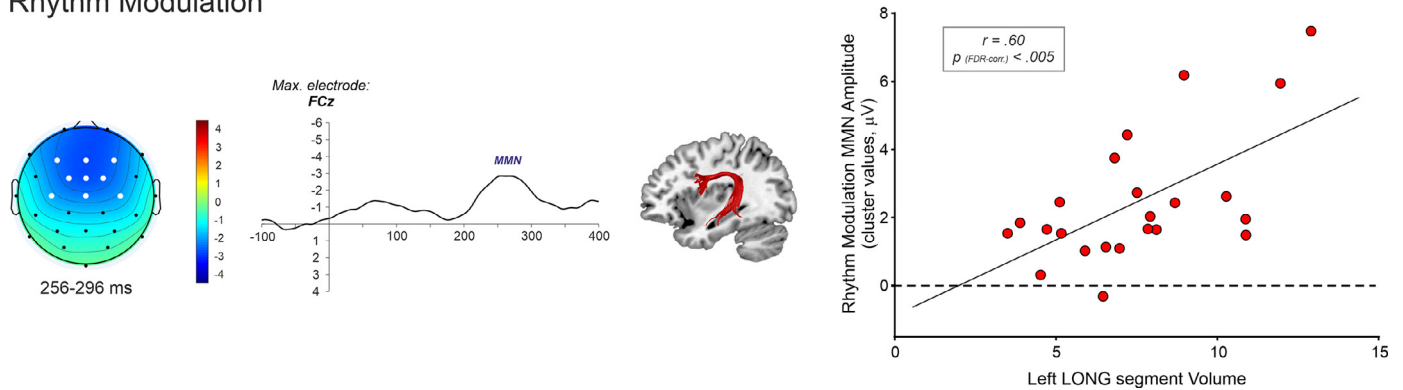
3.3. EEG – DTI correlations

3.3.1. High-level deviants

The only finding robust enough to survive the FDR-correction for multiple comparisons corresponded to the relationship between the cluster values of the MMN amplitude for detecting Rhythm modulation (cluster encompassing F3, Fz, F4, FC1, FCz, FC2, C3, Cz, and C4 electrodes, at 256–296 ms after deviant presentation) and the volume in the left AF long segment ($r = 0.60$, uncorrected $p = .002$, FDR-corrected $p = .024$). Thus, larger volume of the AF long segment on the left hemisphere was related to larger MMN amplitude for rhythmic changes. See **Fig. 4**.

Fig. 3. Deviant–standard difference waveforms and raster plots for the six types of deviants for all participants ($n = 26$). Difference waveforms show the electrodes included in the significant cluster in each condition (i.e., F3, Fz, F4, FC1, FCz, FC2, C3, Cz, C4 for all MMN components; Fz, FCz, Cz for Timbre Deviation's P3a component; and FC1, FCz, FC2, C3, Cz, C4, CP1, CP2 for Rhythm Mistake/Timing Delay's P3a component). Raster plots show the time window and electrodes for which a significant response was found for each condition (if any), with *t*-values color-coded according to the scale at the right side of the raster plot.

Fig. 4. Topography and scatterplot corresponding to the DTI–EEG significant FDR-corrected correlation for High-level deviants. From left to right: topography with white dots highlighting the electrodes pertaining to the significant cluster found; response to Rhythm modulation deviant at FCz, the electrode showing the maximum *t*-value within the selected time-window; schematic depiction of a left long segment superposed on a T1 template image; scatterplot showing the significant correlation between MMN amplitude values within the cluster and the volume of the left long segment. Pearson correlation coefficients and p-values are provided. Abbreviations: MMN, mismatch negativity; FDR, false discovery ratio.

Similarly, a significant uncorrected trend was observed for the relationship between the MMN amplitude cluster–values of the Melody modulation (cluster encompassing F3, Fz, F4, FC1, FCz, FC2, C3, Cz, and C4 electrodes, at 80–120 ms after deviant presentation) and the volume in the right Anterior segment ($r = 0.50$, uncorrected $p = .02$, FDR-corrected $p = .180$), meaning that larger volume of the right hemisphere AF anterior segment predicted better automatic detection of melody modulations. See **Fig. S1**, in the Supplementary Material.

No further significant correlations or significant uncorrected trends were found for the variable MMN latency for either melody or rhythm modulations.

3.3.2. Low-level deviants

No correlations between the low-level deviants and the AF traits survived FDR correction. However, some significant uncorrected trends were found for the correlations between MMN latency for Timbre deviants and the volume in the left AF long ($r = -.48$, uncorrected $p = .021$, FDR-corrected $p = .149$) and left AF anterior ($r = 0.44$, uncorrected $p = .038$, FDR-corrected $p = .152$) segments, and in the right AF posterior segment ($r = 0.57$, uncorrected $p = .005$, FDR-corrected $p = .120$). In other words, the larger the volume in the left long segment, the shorter the peak latency and, thus, the faster the pre-attentive detection, whereas the larger the volume in the indirect segments of the AF bilaterally, the slower the MMN responses for Timbre deviants.

A trend was also found for the correlation between P3a latency for Timbre deviants and the volume of the right posterior segment ($r = 0.45$, uncorrected $p = .031$, FDR-corrected $p = .149$), so the greater the volume in the temporo-parietal branch of the AF, the faster the attentional capture of timbre changes in the melodic stream.

Finally, P3a latency for Rhythm Mistake showed a trend when correlated with left long volume ($r = -0.50$, uncorrected $p = .014$, FDR-corrected $p = .504$), meaning that the smaller the volume values on the left long segment, the faster the attentional capture of Rhythm mistakes.

No further significant correlations with low-level deviant variables (i.e., MMN amplitude for Timbre deviants; MMN amplitude or latency, or P3a amplitude for Rhythm mistake deviants) were found. See **Fig. S2**, in the Supplementary Material, for more details regarding these results.

Since the proportion of men/women in our sample was quite unbalanced (17 out of 23 were women) and because age and sex have been consistently described to affect brain morphology and architecture (Budisavljevic et al., 2015; Catani et al., 2007; Hsu et al., 2008; Lebel and Beaulieu, 2011), we repeated the EEG–DTI correlation analysis controlling for these two factors. However, results remained similar: the only significant finding robust enough to survive the FDR correction for multiple comparisons was the correlation between the volume values of the left long segment and the MMN amplitude cluster–values for the rhythm modulation deviants, and the rest of trends remained as such.

4. Discussion

In the present study, we aimed to explore the relationship between the MMN, a neurophysiological marker of automatic auditory change detection, and the macrostructural properties of the dorsal white-matter pathway connecting potential cortical sources of this ERP component in a sample of 26 healthy non-musicians. The main finding of the present study is a robust association between the volume of the left long segment and the amplitude of the MMN to rhythm modulations. This finding was accompanied by several trends observed between dorsal structural connectivity markers and MMN/P3a indexes for other types of sound deviants (i.e., melody modulations, timbre deviant, timing delay/rhythm mistake conditions). Results are discussed below in the context of the networks involved in auditory processing, highlighting the concept of shared resources for processing language and music.

The association between pre-attentive rhythm-modulation detection and the macrostructure of the left long segment of the AF is in agreement with previous research showing that rhythm perception recruits a bilateral brain network involving both left and right auditory cortices, inferior parietal, premotor and frontal regions (Grahn and Brett, 2007; Lappe et al., 2013; Strauß et al., 2014). This network clearly overlaps with the auditory-motor dorsal stream (Hickok and Poepel, 2007; Rauschecker and Scott, 2009; Patel, 2014; Vaquero et al., 2017, 2018), as well as with the cortical MMN-source network described for acoustic change detection (Doeller et al., 2003; Lappe et al., 2013;

Szycik et al., 2013; Patel and Iversen, 2014). The left lateralization of this result is supported by the specialization of left auditory regions in detecting rapid timing changes in auditory stimuli (Zatorre et al., 1992, 2002; Poeppel, 2003; Albouy et al., 2020). The result could also be arguably driven by the larger volume of left long segment typically exhibited in right-handers and present in our sample (see **Fig. S3**; Powell et al., 2006(Powell, 2006), Catani et al., 2007; Rodrigo et al., 2007(Rodrigo, 2007); Lebel and Beaulieu, 2009; Häberling et al., 2013(Häberling, 2013); Tak et al., 2016(Tak, 2016)). However, we hypothesize that it is the specialization of left auditory regions in processing timing properties / changes of auditory stimuli (Zatorre et al., 1992, 2002; Poeppel, 2003; Friederici and Alter, 2004; Giraud et al., 2007) what is behind the relationship found for detection of rhythmic deviants and the white matter macrostructure of the left fronto-temporal (auditory-motor) segment of the AF. Also, we recently observed that differences in the volume of the right AF as a whole were associated with faster learning rate in a melody task, and differences in volume of the right anterior segment predicted improvements in synchronization during a rhythm learning task (Vaquero et al., 2018). Discrepancies between the present study and the previous one centered on music learning might be mainly due to differences in the focus of attention and the characteristics of the task: passive automatic detection of acoustic deviants, vs. voluntary attention directed towards a rhythmic learning task requiring active auditory-to-motor transformations and self-monitoring. Another possible explanation could be related to rhythm being an important component during speech perception, which could explain the strong left-lateralization observed in the present study for detection of rhythm modulations by using a language-specialized tract. Furthermore, Vuust et al. (2005) showed that rhythm cues elicited similar responses in the left hemisphere, but that musicians showed greater strength in the left than in the right hemisphere when compared to non-musicians. This may also suggest that different levels of expertise or casual experience within our non-musician participants could enhance different brain regions. Importantly, our both studies point out the crucial role of AF in rhythm perception and rhythm learning. The separation of the MMN neural sources from the left and the right temporal cortices and the exploration of other potential neural generators would bring further evidence for the connections involved in this phenomenon. This would be an interesting future direction to perform using magnetoencephalographic (MEG) techniques with a whole-head device, expanding some previous reports with simpler paradigms (Tervaniemi et al., 1999).

Anatomical individual differences in non-musicians in the structural connectivity of the left dorsal stream (DTI measure) were associated with enhanced brain responses regarding rhythm perception (MMN). As mentioned in the introduction, ERPs are elicited by the synchronic activity of large neuronal groups (Elul, 1971; Purpura, 1959; Varela et al., 2001). Individual differences in the underlying white-matter structural connectivity of ERP neural generators might lead to differences in the amplitude morphology or latency of the ERPs. Further, these structural-functional relationships might reflect genetic predispositions or be the consequence of experience-dependent changes (Demerens et al., 1996(Demerens, 1996); Fields, 2005), most probably associated with increased monitoring of the environment for detecting unpredicted relevant sensory changes. Interestingly, the predominant leftward lateralization of the relationship encountered here might point to the possible commonality with language processing cortical mechanisms (Patel, 2010) which could have fine-tuned this network for better detecting rhythm deviants, as well as for monitoring relevant speech information. Despite being all non-musicians, life-time experiences in other domains related to auditory-motor integration, such as speech processing, could be partly responsible of the information transmission efficiency within the left dorsal network. The efficiency shown here in the neuroanatomical circuit involved in automatic deviant sound detection (especially of relevant rhythm changes) might therefore be a consequence of shared resources across music and language domains. Thus, our findings may be the result of specific changes at the level of the aver-

age synaptic input to certain regions in the dorsal circuit (Fields, 2005; Ullén, 2009). These effects could include myelination, changes in thickness and morphology of the myelin sheaths, changes in oligodendrocyte and astrocyte density, and modifications of the vasculature architecture within or close to the tracts, which are all possible biological mechanisms behind the tract volume measurements obtained with diffusion imaging (Juraska and Marham, 2004; Tham et al., 2011; Zatorre et al., 2012; Frintrop et al., 2018; Zhang et al., 2017).

Although non-corrected for multiple comparisons, other trends were encountered, suggesting, as well, an important role for the AF in auditory change detection. Specifically, we observed that melody modulation was slightly related to the macrostructural connectivity of the right anterior segment. These results are in line with previous reports showing that melody-related traits (such as prosody, contour, pitch) are highly lateralized to the right hemisphere (Poeppel, 2003; Boemio et al., 2005; Zatorre et al., 1992, 2002, 2007; Sammler et al., 2015; Vaquero et al., 2018). Moreover, greater volume values in the left long segment were related to faster detection of timbre deviants (i.e., MMN latency), while the macrostructural properties of the indirect segments in both hemispheres (i.e., left anterior, right posterior) showed a positive relationship with MMN latency for these same deviants. Attentional capture towards timbre deviants (measured via P3a latencies) also showed a positive association with the connectivity of the right posterior segment of the AF. Taken together, these results may suggest a potential important role for the left long segment in detecting variation in timbre, whereas the indirect segments may not play an important part in timbre change detection. Finally, faster attentional capture towards rhythm mistakes reflected by P3a latencies was related with larger volume values in the left long segment, which might support our main result concerning the left long segment in detecting rhythmic changes, probably due to the specialization of left auditory regions in detecting timing properties of the stimulus (Zatorre et al., 1992, 2002; Poeppel, 2003; Albouy et al., 2020). Summing up, although the strongest finding concerns the relationship of the left fronto-temporal (auditory-motor) connection with the ability to detect modulations in rhythm, our uncorrected trends suggest that this same left auditory-motor tract may be involved in detecting timbre and timing-delay changes within a melody, while the right AF fronto-parietal connections may be important for detecting violations in melodic traits of the stimuli (see **Fig. S4** for a summary of results).

Overall, our findings provide further evidence of the role of the AF in supporting the direct connection between the two main brain regions proposed to be the neural generators of the MMN component, organized in a hierarchical structure in which the temporal generators sustain a sensory role whereas prefrontal sources might be involved in regulating automatic attention-switching processes (Giard et al., 1990, 1995; Deouell et al., 1998; Alain et al., 1998; Giard et al., 1990). Following this idea, the right IFG has been recently proposed to be responsible for integrating the information about the predictions and the confidence in those predictions during probabilistic learning (Meyniel et al., 2017). Finally, our results could be suggesting a modular kind of processing of rhythmic (left lateralized) and melodic stimulus (right lateralized), adding potential interesting information to this debate ((Brown et al., 2015); Phillips-Silver et al., 2013(Phillips-Silver, 2013); Sihvonen et al., 2016(Sihvonen, 2016), 2017(Sihvonen, 2017)). However, we acknowledge that a greater sample could have granted us a stronger and more reliable statistical power, clarifying which of the observed trends could be significant correlations. Nonetheless the fact that only one parameter of white-matter architecture was reliably related with only one type of pre-attentive deviant detection suggests an actual and strong link between volume of the left long segment and amplitude of detection of rhythm modulation deviants, and the fact that controlling by age and sex do not change the result strengthen this idea.

A bigger sample might have allowed, as well, a possible three-way significant correlation between brain structure, automatic acoustic-deviant detection, and cognitive or music learning variables, which would have increased the relevance of our results. Previous reports

have indeed shown interesting relationship between the MMN brain response and amount of music experience, and individual differences in sound changes detection in language- and music-related stimuli (Amenedo and Escera, 2000; Novitski et al., 2004; Shestopalova et al., 2018; Tervaniemi et al., 2014, 2016; Haumann et al., 2018). The lack of correlation with behavioural variables in the present study is indeed unfortunate, but we hope it would motivate future interesting studies. Moreover, subsequent studies should include other auditory-, music- and language-related white matter pathways in order to explore in more detail the role played by each one of them, in addition to the involvement of the AF. Lastly, because the EEG signals primarily reflect summed postsynaptic potentials recorded from cortical pyramidal neurons, they indirectly reflect the inherent dynamics of the circuits connecting separated brain regions. Notice, however, that we focused our analysis in time-related averaged EEG activity. Since oscillatory activity is a better index of functional integration of large cortical networks associated to coordinate neural populations (Engel et al., 2001), the coupling between this measure with individual differences in white-matter structure of the underlying physical pathways might provide very relevant information.

In conclusion, to the best of our knowledge, this is the first study exploring the relationship between the neurophysiological markers of automatic auditory change detection and the white-matter macrostructural organization of fiber tracts by using DTI-tractography methods. Although exploratory, we provided here first evidence on the constraints imposed by individual differences in neuroanatomical characteristics of the dorsal auditory-motor stream in pre-attentive auditory deviance detection as measured by the MMN component. We conclude that left fronto-temporal connections seem to play an important role in automatic rhythm-deviant detection. Furthermore, linguistic or informal musical exposure are potential experiences responsible for fine-tuning this network and, thus, may underlie the individual differences supporting the detection advantage

Author contributions

Lucía Vaquero: Conceptualization, Formal analysis, Investigation, Writing–Original Draft, Writing–Review & Editing, Visualization, Project administration

Neus Ramos-Escobar: Formal analysis, Investigation, Data curation, Writing–Original Draft, Writing–Review & Editing

David Cucurell: Formal analysis, Writing–Review & Editing

Clément François: Conceptualization, Writing–Original Draft, Writing–Review & Editing

Vesa Putkinen: Validation, Writing–Review & Editing

Emma Segura: Formal analysis, Data curation, Writing–Review & Editing

Minna Huotilainen: Methodology, Writing–Review & Editing

Virginia Penhune: Writing–Original Draft, Writing–Review & Editing

Antoni Rodríguez-Fornells: Conceptualization, Writing–Original Draft, Writing–Review & Editing, Supervision, Funding acquisition.

Data & code availability statement

We would like to make available to the readers all the data discussed in the paper; however, we should comply with the Ethics Committee of the Hospital Universitari de Bellvitge, which means that only the data for those participants who specifically agreed to secondary use of data in the consent form used in the experiment will be made available (after an anonymization process).

Acknowledgments

Supplementary materials

Supplementary material associated with this article can be found, in the online version, at doi:10.1016/j.neuroimage.2021.117759.

References

Alain, C., Hargrave, R., Woods, D.L., 1998. Processing of auditory stimuli during visual attention in patients with schizophrenia. Biol. Psychiatry 44 (11), 1151–1159.

Albouy, P., Benjamin, L., Morillon, B., Zatorre, R.J., 2020. Distinct sensitivity to spectrotemporal modulation supports brain asymmetry for speech and melody. Science 367 (6481), 1043–1047.

Alho, K., Woods, D.L., Algazi, A., Knight, R.T., Näätänen, R., 1994. Lesions of frontal cortex diminish the auditory mismatch negativity. Electroencephalogr. Clin. Neurophysiol. 91 (5), 353–362.

Alho, K., Tervaniemi, M., Huotilainen, M., Lavikainen, J., Tiitinen, H., Ilmoniemi, R.J., Knuutila, J., Näätänen, R., 1996. Processing of complex sounds in the human auditory cortex as revealed by magnetic brain responses. Psychophysiology 33 (4), 369–375.

Amenedo, E., Escera, C., 2000. The accuracy of sound duration representation in the human brain determines the accuracy of behavioural perception. Eur. J. Neurosci. 12 (7), 2570–2574.

Behrens, T.E., Johansen-Berg, H., 2005. Relating connectional architecture to grey matter function using diffusion imaging. Philos. Trans. R. Soc. Lond. B Biol. Sci. 360 (1457), 903–911.

Berti, S., 2013. The role of auditory transient and deviance processing in distraction of task performance: a combined behavioural and event-related brain potential study. Front. Hum. Neurosci. 7, 352.

Blair, R.C., Karniski, W., 1993. An alternative method for significance testing of waveform difference potentials. Psychophysiology 30 (5), 518–524.

Boemio, A., Fromm, S., Brain, A., Peoppel, D., 2005. Hierarchical and asymmetric temporal sensitivity in human auditory cortices. Nat. Neurosci. 8 (3), 389–395.

Brown, R.M., Zatorre, R.J., Penhune, V., 2015. Expert music performance: cognitive, neural, and developmental bases. Prog. Brain Res. 217, 57–86.

Budisavljevic, S., Dell'Acqua, F., Rijsdijk, F.V., Kane, F., Picchioni, M., MCGuire, P., Toulopoulou, T., Georgiades, A., Kalidindi, S., Kravariti, E., Murray, R.M., Murphy, D.G., Craig, M.C., Catani, M., 2015. Age-related differences and heritability of the Perisylvian language networks. J. Neurosci. 35 (37), 12625–12634.

Campos-Arteaga, G., Forcato, C., Wainstein, G., Lagos, R., Palacios-García, I., Artigas, C., Morales, R., Pedreira, M.E., Rodríguez, E., 2020. Differential neurophysiological correlates of retrieval of consolidated and reconsolidated memories in humans: an ERP and pupillometry study. Neurobiol. Learn. Mem. 174, 107279. doi:10.1016/j.nlm.2020.107279.

Cardenas, V.A., Chao, L.L., Blumfeld, R., Song, E., Meyerhoff, D.J., Weiner, M.W., Studholme, C., 2005. Using automated morphometry to detect associations between ERP latency and structural brain MRI in normal adults. Hum. Brain Mapp. 25 (3), 317–327.

Catani, M., Jones, D.K., ffytche, D.H., 2005. Perisylvian language networks of the human brain. Ann. Neurol. 57 (1), 8–16.

Catani, M., Allin, M.P., Husain, M., Pugliese, L., Mesulam, M.M., Murray, R.M., Jones, D.K., 2007. Symmetries in human brain language pathways correlate with verbal recall. Proc. Natl. Acad. Sci. USA 104 (43), 17163–17168.

Catani, M., Mesulam, M., 2008. The arcuate fasciculus and the disconnection theme in language and aphasia: history and current state. Cortex 44 (8), 953–961.

Cowan, N., Winkler, I., Teder, W., Näätänen, R., 1993. Memory prerequisites of the mismatch negativity in the auditory event-related potential (ERP). J. Exp. Psychol/ Learn. Mem. Cognit. 19, 909–921.

Cunillera, T., Càmara, E., Toro, J.M., Marco-Pallarés, J., Sebastián-Galles, N., Ortiz, H., Pujol, J., Rodríguez-Fornells, A., 2009. Time course and functional neuroanaotmy of speech segmentation in adults. Neuroimage 48 (3), 541–553.

Demerens, 1996. Induction of myelination in the central nervous system by electrical activity. Proc. Natl. Acad. Sci. U.S.A. doi:10.1073/pnas.93.18.9887.

Deouell, L.Y., Bentin, S., Giard, M.H., 1998. Mismatch negativity in dichotic listening: evidence for interhemispheric difference and multiple generators. Psychophysiology 35 (4), 355–365.

Doeller, C.F., Opitz, B., Mecklinger, A., Krick, C., Reith, W., Schröger, E., 2003. Prefrontal cortex involvement in preattentive auditory deviance detection: neuroimaging and electrophysiological evidence. Neuroimage 20 (2), 1270–1282.

Elul, R., 1971. The genesis of the EEG. Int. Rev. Neurobiol. 15, 227–272.

Engel, A.K., Fries, P., Singer, W., 2001. Dynamic predictions: oscillations and synchrony in top-down processing. Nat. Rev. Neurosci. 2 (10), 704–716.

Escera, C., Alho, K., Schröger, E., Winkler, I., 2000. Involuntary attention and distractibility as evaluated with event-related potentials. Audiol. Neurootol. 5 (3–4), 151–166.

Fields, R.D., 2005. Myelination: an overlooked mechanism of synaptic plasticity? Neuroscientist 11, 528–531.

Fields, R.D., 2008. White matter in learning, cognition and psychiatric disorders. Trends Neurosci. 31 (7), 361–370.

Friederici, A.D., Alter, K., 2004. Lateralization of auditory language functions: a dynamic pathway model. Brain Lang. 89 (2), 267–276.

Friedman, D., Cycowicz, Y.M., Gaeta, H., 2001. The novelty P3: an event-related brain potential (ERP) sign of the brain's evaluation of novelty. Neurosci. Biobehav. Rev. 25 (4), 355–373.

Frintrop, L., Liesbrock, J., Paulukat, L., Johann, S., Kas, M.J., Tolba, R., Heussen, N., Neulen, J., Konrad, K., Herpertz-Dahlmann, B., Beyer, C., Seitz, J, 2018. Reduced astrocyte density underlying brain volume reduction in activity-based anorexia rats. World J. Biol. Psychiatry 19 (3), 225–235.

Frodl-Bauch, T., Kathmann, N., Möller, H.J., Hegerl, U., 1997. Dipole localization and test-retest reliability of frequency and duration mismatch negativity generator processes. Brain Topogr. 10 (1), 3–8.

Giard, M.H., Perrin, F., Pernier, J., Bouchet, P., 1990. Brain generators implicated in the processing of auditory stimulus deviance: a topographic event-related potential study. Psychophysiology 27 (6), 627–640.

Fujioka, 2004. Musical training enhances automatic encoding of melodic contour and interval structure.. Journal of Cognitive Neuroscience doi:10.1162/0898929041502706.

Giard, M.H., Lavikahen, J., Reinikainen, K., Perrin, F., Bertrand, O., Pernier, J., Näätänen, R., 1995. Separate representation of stimulus frequency, intensity, and duration in auditory sensory memory: an event-related potential and dipole-model analysis. J. Cognit. Neurosci. 7 (2), 133–143.

Giraud, A.L., Kleinschmidt, A., Poeppel, D., Lund, T.E., Frackowiak, R.S., Laufs, H., 2007. Endogenous cortical rhythms determine cerebral specialization for speech perception and production. Neuron 56 (6), 1127–1134.

Grahn, J.A., Brett, M., 2007. Rhythm and beat perception in motor areas of the brain. J. Cognit. Neurosci. 19 (5), 893–906.

Grimm, S., Escera, C., 2012. Auditory deviance detection revisited: evidence for a hierarchical novelty system. Int. J. Psychophysiol. 85 (1), 88–92.

Groppe, D.M., Urbach, T.P., Kutas, M., 2011. Mass univariate analysis of event-related brain potentials/fields I: a critical tutorial review. Psychophysiology 48 (12), 1711–1725.

Grotheer, M., Kovács, G., 2016. Can predictive coding explain repetition suppression? Cortex 80, 113–124.

Häberling, 2013. Asymmetries of the Arcuate Fasciculus in Monozygotic Twins: Genetic and Nongenetic Influences.. PLoS ONE doi:10.1371/journal.pone.0052315.

Halgren, E., Baudena, P., Clarke, J.M., Heit, G., Marinkovic, K., Devaux, B., Vignal, J.P., Biraben, A., 1995. Intracerebral potentials to rare target and distractor auditory and visual stimuli. I. Superior temporal plane and parietal lobe. Electroencephalogr. Clin. Neurophysiol. 94, 191–220.

Haumann, N.T., Vuust, P., Bertelsen, F., Garza-Villareal, E.A., 2018. Influence of musical enculturation on brain responses to metric deviants. Front. Neurosci. 12, 218.

Hemmelmann, C., Horn, M., Reiterer, S., Schack, B., Susse, T., Weiss, S., 2004. Multivariate tests for the evaluation of high-dimensional EEG data. J. Neurosci. Methods 139 (1), 111–120.

Hickok, G., Poeppel, D., 2007. The cortical organization of speech processing. Nat. Rev. Neurosci. 8 (5), 393–402.

Horváth, J., Winkler, I., Bendixen, A., 2008. Do N1/MMN, P3a, and RON form a strongly coupled chain refleting the three stages of auditory distraction? Biol. Psychol. 79 (2), 139–147.

Horváth, J., Müller, D., Weise, A., Schröger, E., 2010. Omission mismatch negativity builds up late. Neuroreport 21 (7), 537–541.

Hsu, J.L., Leemans, A., Bai, C.H., Lee, C.H., Tsai, Y.F., Chiu, H.C., Chen, W.H., 2008. Gender differences and age-related white matter changes of the human brain: a diffusion tensor imaging study. Neuroimage 39 (2), 566–577.

James, C.E., Oechslin, M.S., Van De Ville, D., Hauert, C.A., Descloux, C., Lazeyras, F., 2014. Musical training intensity yields opposite effects on grey matter density in cognitive versus sensorimotor networks. Brain Struct. Funct. 219 (1), 353–366.

Jasper, H.H., 1958. The ten twenty electrode system of the international federation. Electroencephalogr. Clin. Neurophysiol. 10, 371–375.

Juraska, J.M., Markham, J.A., 2004. The cellurlar basis for volume changes in the rat cortex during puberty: white and gray matter. Ann. N. Y. Acad. Sci. 1021, 431–435.

Kilner, J.M., 2013. Bias in a common EEG and MEG statistical analysis and how to avoid it. Clin. Neurophysiol. 124 (10), 2062–2063.

Kleber, B., Zeitouni, A.G., Friberg, A., Zatorre, R.J., 2013. Experience-dependent modulation of feedback integration during singing: role of the right anterior insula. J. Neurosci. 33 (14), 6070–6080.

V Koelsch, S., Fritz, T., Crammon, D.Y., Müller, K., Friederici, A.D., 2006. Investigating emotion with music: an fMRI study. Hum. Brain Mapp. 27 (3), 239–250.

Koelsch, S., Vuust, P., Friston, K., 2018. Predictive processes and the peculiar case of music. Trends Cognit. Sci. (Regul. Ed.).

Lappe, C., Steinsträter, O., Pantev, C., 2013. Rhythm and melodic deviations in musical sequences recruit different cortical areas for mismatch detection. Front. Hum. Neurosci. 7, 260.

Lebel, C., Beaulieu, C., 2009. Lateralization of the arcuate fasciculus from childhood to adulthood and its relation to cognitive abilities in children. Hum. Brain Mapp. 30 (11), 3563–3573.

Lebel, C., Beaulieu, C., 2011. Longitudinal development of human brain wiring continues from childhood into adulthood. J. Neurosci. 31 (30), 10937–10947.

López-Barroso, D., Catani, M., Ripollés, P., Dell'Acqua, F., Rodríguez-Fornells, A., de Diego-Balaguer, R., 2013. Word learning is mediated by the left arcuate fasciculus. Proc. Natl. Acad. Sci. USA 110 (32), 13168–13173.

Loui, P., 2015. A dual-stream neuroanatomy of singing. Music Percept. 32 (3), 232–241.

Maess, B., Jacobsen, T., Schröger, E., Friederici, A.D., 2007. Localizing pre-attentive memory-based comparison: magnetic mismatch negativity to pitch change. Neuroimage 37 (2), 561–571.

Mamiya, P.C., Richards, T.L., Coe, B.P., Eichler, E.E., Kuhl, P.K., 2016. Brain white matter structure and COMT gene are linked to second-language learning in adults. Proc. Natl. Acad. Sci. USA 113 (26), 7249–7254.

Manly, B.F.J. 1997. Randomization, Bootstrap, and Monte Carlo Methods in Biology, 2nd ed. Chapman & Hall, London.

Meyniel, F., Dehaene, S., 2017. Brain networks for confidence weigthing and hierarchical inference during probabilistic learning. Proc. Natl. Acad. Sci. U.S.A. 114 (19), E3859–E3868.

Näätänen, R., Gaillard, A.W., Mäntysalo, S., 1978. Early selective-attention effect on evoked potential reinterpreted. Acta Psychol. 42 (4), 313–329.

Näätänen, R., Lehtokoski, A., Lennes, M., Cheour, M., Huotilainen, M., Iivonen, A., Vainio, M., Alku, P., Ilmoniemi, R.J., Luuk, A., Allik, J., Sinkkonen, J., Alho, K., 1997. Language-specific phoneme representations revealed by electric and magnetic brain responses. Nature 385 (6615), 432–434.

Näätänen, R., Jacobsen, T., Winkler, I., 2005. Memory-based or afferent processes in mismatch negativity (MMN): a review of the evidence. Psychophysiology 42 (1), 25–32.

Näätänen, R., Paavilainen, P., Rinne, T., Alho, K., 2007. The mismatch negativity (MMN) in basic research of central auditory processing: a review. Clin. Neurophysiol. 118 (12), 2544–2590.

Nager, W., Teder-Sälejärvi, W., Kunze, S., Münte, T.F., 2003. Preattentive evaluation of multiple perceptual streams in human audition. Neuroreport 14 (6), 871–874.

Nikjeh, 2009. Preattentive cortical-evoked responses to pure tones, harmonic tones, and speech: Influence of music training.. Ear and Hearing doi:10.1097/AUD.0b013e3181a61bf2.

Novitski, N., Tervaniemi, M., Huotilainen, M., Näätänen, R., 2004. Frequency discrimination at different frequency levels as indexed by electrophysiological and behavioral measures. Brain Res. Cognit. Brain Res. 20 (1), 26–36.

Opitz, B., Rinne, T., Mecklinger, A., von Cramon, D.Y., Schröger, E., 2002. Differential contribution of frontal and temporal cortices to auditory change detection: fMRI and ERP results. Neuroimage 15 (1), 167–174.

Paraskevopoulos, 2012. Statistical learning effects in musicians and non-musicians: An MEG study.. Neuropsychologia doi:10.1016/j.neuropsychologia.2011.12.007.

Patel, A.D., 2014. Can nonlinguistic musical training change the way the brain processes speech? The expanded OPERA hypothesis. Hear. Res. 308, 98–108.

Patel, A.D., Iversen, J.R., 2014. The evolutionary neuroscience of musical beat perception: the action simulation for auditory prediction (ASAP) hypothesis. Front. Syst. Neurosci. 8, 57.

Peretz, I., Champod, A.S., Hyde, K., 2003. Varieties of musical disorders. Ann. N. Y. Acad. Sci. 999 (1), 58–75.

Petersen, B., Friis-Andersen, A.S., Haumann, N.T., Højlund, A., Dietz, M.J., Michel, F., Riis, S.K., Brattico, E., Vuust, P., 2020. The CI MuMuFe – a new MMN paradigm for measuring music discrimination in electric hearing. Front. Neurosci. 14, 2.

Phillips-Silver, 2013. Amusic does not mean unmusical: Beat perception and synchronization ability despite pitch deafness.. Cognitive Neuropsychology doi:10.1080/02643294.2013.863183.

Picton, T.W., Alain, C., Otten, L., Ritter, W., Achim, A., 2000. Mismatch negativity: different water in the same river. Audiol. Neurootol. 5 (3–4), 111–139.

Poeppel, D., 2003. The analysis of speech in different temporal integration windows cerebral lateralization as 'asymmetric sampling in time. Speech Commun. 41, 245–255.

Powell, 2006. Hemispheric asymmetries in language-related pathways: A combined functional MRI and tractography study.. NeuroImage doi:10.1016/j.neuroimage.2006.03.011.

Purpura, D.P., 1959. Nature of electrocortical potentials and synaptic organizations in cerebral and cerebellar cortex. Int. Rev. Neurobiol. 1, 47–163.

Putkinen, V., Tervaniemi, M., Saarikivi, K., de Vent, N., Huotilainen, M., 2014. Investigating the effects of musical training on functional brain development with a novel melodic MMN paradigm. Neurobiol. Learn. Mem. 110, 8–15.

Rauschecker, J.P., Scott, S.K., 2009. Maps and streams in the auditory cortex: nonhuman primates illuminate human speech processing. Nat. Neurosci. 12 (6), 718–724.

Rodrigo, 2007. Human subinsular asymmetry studied by diffusion tensor imaging and fiber tracking.. American Journal of Neuroradiology doi:10.3174/ajnr.A0584.

Rodríguez-Fornells, A., Cunillera, T., Mestres-Missé, A., de Diego-Balaguer, R., 2009. Neurophysiological mechanisms involved in language learning in adults. Philos. Trans. R. Soc. B Biol. Sci. 364 (1536), 3711–3735.

Rykhlevskaia, E., Gratton, G., Fabiani, M., 2008. Combining structural and functional neuroimaging data for studying brain connectivity: a review. Psychophysiology 45 (2), 173–187.

Sammler, D., Koelsch, S., Friederici, A.D., 2011. Are left fronto-temporal brain areas a prerequisite for normal music-syntactic processing? Cortex 47 (6), 659–673.

Sammler, D., Grosbras, M.H., Anwander, A., Bestelmeyer, P.E., Belin, P., 2015. Dorsal and ventral pathways for prosody. Curr. Biol. 25 (23), 3079–3085.

Sánchez-Carmona, A.J., Albert, J., Hinojosa, J.A., 2016. Neural and behavioral correlates of selective stopping: evidence for a different strategy adoption. Neuroimage 139, 279–293.

Scheer, M.-., Bülthoff, H.H., Chuang, L.L., 2016. Steering demands diminish the early-P3, Late-P3 and RON components of the event-related potential of task irrelevant environmental sounds. Front. Hum. Neurosci. 10, 73.

Shestopalova, L.B., Petropavolovskaia, E.A., Semenova, V.V., Nikitin, N.I., 2018. Mismatch negativity and psychophysical detection of rising and falling intensity sounds. Biol. Psychol. 133, 99–111.

Sihvonen, 2016. Neural basis of acquired amusia and its recovery after stroke.. Journal of Neuroscience doi:10.1523/JNEUROSCI.0709-16.2016.

Sihvonen, 2017. Revisiting the neural basis of acquired amusia: Lesion patterns and structural changes underlying amusia recovery.. Frontiers in Neuroscience doi:10.3389/fnins.2017.00426.

Smith, S.M., 2002. Fast robust automated brain extraction. Hum. Brain Mapp. 17 (3), 143–155.

Smith, S.M., Jenkinson, M., Woolrich, M.W., Beckmann, C.F., Behrens, T.E., Johansen-Berg, H., Bannister, P.R., De Luca, M., Drobnjak, I., Flitney, D.E., Niazy, R.K., 2004. Advances in functional and structural MR image analysis and implementation as FSL. Neuroimage 23, S208–S219.

Strauß, A., Kotz, S.A., Scharinger, M., Obleser, J., 2014. Alpha and theta brain oscillations index dissociable processes in spoken word recognition. Neuroimage 97, 387–395.

Sui, J., Huster, R., Yu, Q., Segall, J.M., Calhoun, V.D., 2014. Function-structure associations of the brain: evidence from multimodal connectivity and covariance studies. Neuroimage 102 (Pt 1), 11–23.

Szycik, G.R., Stadler, J., Brechmann, A., Münte, T.F., 2013. Preattentive mechanisms of change detection in early auditory cortex: a 7 Tesla fMRI study. Neuroscience 253, 100–109.

Tervaniemi, M., Kujala, A., Alho, K., Virtanen, J., Ilmonen, R.J., Näätänen, R., 1999. Functional specialization of the human auditory cortex in processing phonetic and musical sounds: a magnetoencephalographic (MEG) study. Neuroimage 9 (3), 330–336.

Tak, 2016. Developmental process of the arcuate fasciculus from infancy to adolescence: A diffusion tensor imaging study.. Neural Regeneration Research doi:10.4103/1673-5374.184492.

Tervaniemi, M., Huotilainen, M., Brattico, E., 2014. Melodic multi-feature paradigm reveals auditory profiles in music-sound encoding. Front. Hum. Neurosci. 8, 496.

Tervaniemi, M., Janhunen, L., Kruck, S., Putkinen, V., Huotilainen, M., 2016. Auditory profiles of classical, jazz, and rock musicians: genre-specific sensitivity to musical sound features. Front. Psychol. 6, 1900.

Tham, M.W., Woon, P.S., Sum, M.Y., Lee, T.S., Sim, K., 2011. White matter abnormalities in major depression: evidence from post-mortem, neuroimaging and genetic studies. J. Affect. Disord. 132 (1–2), 26–36.

Thiebaut de Schotten, M., Ffytche, D.H., Bizzi, A., Dell'Acqua, F., Allin, M., Walshe, M., Murray, R., Williams, S.C., Murphy, D.G., Catani, M, 2011. Atlasing location, asymmetry and inter-subject variability of white matter tracts in the human brain with MR diffusion tractography. Neuroimage 54 (1), 49–59.

Ullén, F., 2009. Is activity regulation of late myelination a plastic mechanism in the human nervous system? Neuron Glia Biol. 5, 29–34.

Vaquero, L., Rodríguez-Fornells, A., Reiterer, S.M., 2017. The left, the better: white-matter brain integrity predicts foreign language imitation ability. Cereb. Cortex 27 (8), 3906–3917.

Valdés-Hernández, 2010. White matter architecture rather than cortical surface area correlates with the EEG alpha rhythm. NeuroImage doi:10.1016/j.neuroimage.2009.10.030.

Vaquero, 2020. What you learn & when you learn it: Impact of early bilingual & music experience on the structural characteristics of auditory-motor pathways.. NeuroImage doi:10.1016/j.neuroimage.2020.116689.

Vaquero, L., Ramos-Escobar, N., François, C., Penhune, V., Rodríguez-Fornells, V., 2018. White-matter structural connectivity predicts short-term melody and rhythm learning in non-musicians. Neuroimage 181, 252–262.

Varela, F., Lachaux, J.P., Rodriguez, E., Martinerie, J., 2001. The brainweb: phase synchronization and large-scale integration. Nat. Rev. Neurosci. 2 (4), 229–239.

Virtala, 2014. Musicianship facilitates the processing of Western music chords-An ERP and behavioral study.. Neuropsychologia doi:10.1016/j.neuropsychologia.2014.06.028.

Vuust, 2012. The sound of music: Differentiating musicians using a fast, musical multi-feature mismatch negativity paradigm.. Neuropsychologia doi:10.1016/j.neuropsychologia.2012.02.028.

Vuust, P., Liikala, L., Näätänen, R., Brattico, P., Brattico, E., 2016. Comprehensive auditory discrimination profiles recorded with a fast parametric musical multi-feature mismatch negativity paradigm. Clin. Neurophysiol. 127 (4), 2065–2077.

Vuust, P., Pallesen, K.J., Bailey, C., Van Zuijen, T.L., Gjedde, A., Roepstorff, A., Østergaard, L., 2005. To musicians, the message is in the meter: pre-attentive neuronal responses to incongruent rhythm are left-lateralized in musicians. Neuroimage 24 (2), 560–564.

Westlye, L.T., Walhovd, K.B., Bjørnerud, A., Due-Tønnessen, P., Fjell, A.M., 2009. Error-related negativity is mediated by fractional anisotropy in the posterior cingulate gyrus–a study combining diffusion tensor imaging and electrophysiology in healthy adults. Cereb. Cortex 19 (2), 293–304.

Winkler, I., Denham, S.L., Nelken, I., 2009. Modeling the auditory scene: predictive regularity representations and perceptual objects. Trends Cognit. Sci. 13 (12), 532–540.

Woolrich, M.W., Jbabdi, S., Patenaude, B., Chappell, M., Makni, S., Behrens, T., Beckmann, C., Jenskinson, M., Smith, S.M., 2009. Bayesian analysis of neuroimaging data in FSL. Neuroimage 45, S173–S186.

Zatorre, R.J., Evans, A.C., Meyer, E., Gjedde, A., 1992. Lateralization of phonetic and pitch discrimination in speech processing. Science 256 (5058), 846–849.

Zatorre, R.J., Belin, P., Penhune, V.B., 2002. Structure and function of auditory cortex: music and speech. Trends Cognit. Sci. 6 (1), 37–46.

Zatorre, R.J., Chen, J.L., Penhune, V.B., 2007. When the brain plays music: auditory-motor interactions in music perception and production. Nat. Rev. Neurosci. 8 (7), 547–558.

Zatorre, R.J., Fields, R.D., Johansen-Berg, H., 2012. Plasticity in gray and white: neuroimaging changes in brain structure during learning. Nat. Neurosci. 15 (4), 528–536.

Zhang, Y., Chao, F.L., Zhou, C.N., Jiang, L., Zhang, L., Chen, L.M., Luo, Y.M., Xiao, Q., Tang, Y, 2017. Effects of exercise on capillaries in the white matter of transgenic AD mice. Oncotarget 8 (39), 65860–65875.